2016 24th International Lightning Detection Conference & 6th International Lightning Meteorology Conference
18 - 21 April | San Diego, California, USA

Lightning in Secondary Convection Produced within the Anvil of the the 29-30 May 2012 Supercell Storm during DC3

Donald R. MacGorman
NOAA/National Severe Storms Laboratory
Norman, Oklahoma, USA
e-mail: don.macgorman@noaa.gov

Elizabeth DiGangi
Cooperative Inst. for Mesoscale Meteorological Studies
University of Oklahoma and DOC/NOAA/NSSL
Norman, Oklahoma, USA
e-mail: elizabeth.digangi@noaa.gov

***Abstract*— On 29 May 2012, a tornadic supercell thunderstorm formed near Kingfisher, Oklahoma, within range of the KTLX WSR-88D radar and the Oklahoma Lightning Mapping Array. This study focuses on a ~1.5-hour interval during which secondary convection was initiated and strengthened in the anvil. Horizontally extensive lightning flashes propagated through and were initiated within the anvil during this period and are examined relative to radar reflectivity, radial velocity, and NLDN ground strike points. Flashes were first initiated in the distant anvil when secondary convection formed in the vicinity of the flash initiations as a result of local destabilization produced by evaporative cooling in falling virga, coincident with low-level updrafts from convergence along a surface outflow boundary. The timing of the anvil flash initiations and the charge structure inferred from flashes in the main storm, the anvil, and the secondary anvil convection indicate that charge was generated by the secondary convection.**

Keywords—lightning, electrification, anvil, convection

I. Introduction

Several studies have found that anvils of thunderstorms can contain electric fields strong enough to support or initiate lightning (e.g., Rust et al. 1981, Byrne et al. 1989, Marshall et al. 1989, Bluestein and MacGorman 1998, Dye and Willett 2007). Though anvil lightning is commonplace, especially in supercell thunderstorms, only relatively recently have studies performed detailed analyses of mapped lightning in anvils (e.g. Dye et al. 2007, Kuhlman et al. 2009, Weiss et al. 2012). Kuhlman et al. (2009) and Weiss et al. (2012) documented cloud-to-ground (CG) flashes being initiated and striking ground up to 100 km from the deeper precipitation of the parent storm. Because lightning strikes typically are not expected in this situation, it poses a poorly understood threat to the general public, as well as to commercial and governmental interests.

The source of charge involved in the lightning observed in thunderstorm anvils has been a subject of debate for several years. Dye et al. (2007) and Kuhlman et al. (2009) noted that the source of charge in some anvils is likely similar to the source of charge in the stratiform region of mesoscale convective systems (MCS). Studies of the stratiform precipitation region of MCSs found that the substantial charge advected from the convective cores of thunderstorms likely must be supplemented by in situ non-inductive charging (e.g., Takahashi and Miyawaki 2002, Emersic and Saunders 2010) to provide the charge structures and lightning observed in the distant portions of the stratiform region (Stolzenburg et al. 1994, Schuur and Rutledge 2000). From aircraft flights through anvils, Dye and Willett (2007) noted that localized regions of enhanced electric field in thunderstorm anvils were coincident with localized regions of enhanced radar reflectivity. Weiss et al. (2012) inferred from observations of distant anvils for several supercell storms that the initiation of flashes in the distant anvil appeared to be associated with three charge configurations: (1) an interaction between internal anvil charge and screening layer charge that formed on the upper anvil cloud boundary, (2) charge regions in two anvils having opposite polarities of charge at the same altitude as the anvils from two parent storms merge, and (3) charge associated with downward protrusions of reflectivity in anvils, indicative of falling precipitation.

Weiss et al. (2012) suggested that lightning initiations were associated with downward protrusions of reflectivity in the anvil because charge was being produced locally in secondary convection by a process described by Knight et al (2004), who noted that evaporative cooling of falling precipitation can destabilize the environment locally. However, Weiss et al. (2012) pointed out that, to form convection, the destabilization would need to occur in a region of weak updrafts at lower

This research was supported by NSF grants #1063945 and 1063537 and by NOAA/Office of Oceanic and Atmospheric Research under NOAA-University of Oklahoma Cooperative Agreement #NA11OAR4320072, U.S. Department of Commerce.

levels to overcome the downward inertia of air containing falling precipitation.

The subject of this paper is lightning in the anvil of the 29 May 2012 supercell storm (hereafter called the Kingfisher storm, after a town near which it formed) which was part of a cluster of severe thunderstorms that formed over north-central Oklahoma during the Deep Convective Clouds and Chemistry (DC3) field campaign (Barth et al. 2015). This storm, a prolific lightning producer, was within range of the Oklahoma Lightning Mapping Array (OK-LMA) (MacGorman et al. 2008, Barth et al. 2015) and the Weather Surveillance Radar-1988 Doppler (WSR-88D) radar (Crum and Alberty 1993) at Oklahoma City (KTLX) throughout much of its lifetime, including a period in which it began producing lightning in the anvil. Anvil lightning initially propagated from the parent storm several tens of kilometers into the anvil, but eventually began to be initiated by secondary convection that formed beneath the anvil and struck one of the DC3 aircraft. Thus, this case provides an opportunity to examine anvil lightning in transition between two scenarios and to examine the conditions under which the developing secondary convection was able to produce lightning, a poorly understood process relevant to all activities susceptible to lightning hazards

II. Data and Analysis Methods

A. Lightning

Lightning data for this case are from the OK-LMA, which maps the times and three-dimensional locations at which lightning channel segments emit very high frequency (VHF) radiation (MacGorman et al. 2008, Barth et al. 2015). It computes the time and location of each source from the differences in times at which the signal it radiates arrives at an array of stations in Oklahoma. Details concerning the equipment, data processing techniques, and sources of error for Lightning Mapping Arrays are available in Rison et al. (1999) and Thomas et al. (2004).

Detailed analysis of the LMA data was performed with the XLMA software package developed by researchers at New Mexico Tech. To be considered reliable enough to be used for this study, a VHF source had to be detected by at least seven stations, the reduced $\chi 2$ value of the source computation had to be $\leqslant 2$, and the source height had to be $\leqslant 20$ km, as in previous studies (e.g., Lund et al. 2009, Weiss et al. 2012). All VHF sources which did not appear to be associated with the Kingfisher storm were removed from our analysis. Cloud-to-ground (CG) flashes associated with anvil flashes were identified with data from the National Lightning Detection Network (NLDN) (Cummins and Murphy 2009).

The LMA data were ingested into the Warning Decision Support System - Integrated Information (WDSS-II, Lakshmanan et al. 2007) and then run through the w2lmaflash algorithm to calculate parameters such as flash initiation points (e.g., Herzog 2013). This algorithm calculates flash initiation locations as described by MacGorman et al. (2008) and Lund et al. (2009).

The characteristics of lightning can be used to infer the charge regions involved in lightning flashes from the mapped VHF sources in a flash. From the initiation location, which is in a region of the largest electric fields in a storm, typically between charge regions, flashes propagate bidirectionally into regions of charge, positively charged leaders propagating into and through negative charge and negatively charged leaders propagating into and through positive charge (e.g., Kasemir 1960; Mazur 1989; MacGorman et al. 1981, 2001; Coleman et al. 2003). Negative leaders propagating tend to be more impulsive and thus tend to produce stronger VHF signals and denser VHF sources, so charge regions can be inferred via close examination of leader propagation in the LMA data (e.g., Rust et al. 2005, Wiens et al. 2005, MacGorman et al. 2008, Bruning et al. 2010 }. For this study, the spatial and temporal evolution of flashes in the anvil and in adjacent regions were analyzed to determine the charge distribution in the parent storm, the anvil, and the secondary anvil convection.

B. Radar

Lightning data were overlaid in WDSS-II on data from the Oklahoma City WSR-88D (Crum and Alberty 1993), KTLX. The data were obtained from the National Climactic Data Center (NCDC) and viewed in WDSS-II with the ldm2netcdf algorithm. KTLX had not received the dual-polarimetric upgrade as of May 2012, so only reflectivity and radial velocity data were available for this study. The initiation and track of the secondary convection in the anvil was determined by the WDDS-II w2segmotionll algorithm (Herzog 2013) from the KTLX data. WDDS-II also produced the vertical and horizontal cross sections of KTLX data used extensively in this study to analyze the initiation and evolution of the secondary convection.

III. Observatoins

The Kingfisher storm began at ~21:00 UTC (4:00pm local time) northwest of Oklahoma City, and its first lightning flash occurred at 21:34 UTC. The storm developed two reflectivity cores and underwent a split at ~22:30 UTC. Flash rates and updraft strength began to increase substantially after 23:00 UTC. Anvil flashes and the secondary convection in the anvil were produced after 23:00 UTC, during the Kingfisher storm's intensification phase. This study will focus on the 23:00-00:00 UTC period for analysis.

A. Development of secondary convection

An outflow boundary formed on the eastern flank of the Kingfisher storm and was visible in the KTLX radial velocity data beginning at 22:38 UTC. The boundary propagated eastward with time, as shown in Figure 1. At about 23:11 UTC, WDSS-II detected convective initiation in the anvil along the outflow boundary (Figure 2). The vertical cross-section in Figure 3 (a) shows that convective initiation was approximately collocated with a downward bulge and finger-like tendrils of reflectivity in the anvil along the outflow boundary. By 23:24 UTC, there was at least one notable reflectivity maximum $\geqslant 40$ dBZ visible above the boundary (e.g. Figure 4b).

The descending reflectivity echo became more prominent as time progressed, as larger reflectivities increased and deepened all along the boundary, as shown in Figure 4. At

23:41 UTC, the reflectivity associated with the line of secondary convection began moving eastward off the outflow boundary as the boundary stalled under the anvil (e.g. Figure 2), and the secondar convection eventually broke away from the Kingfisher storm's anvil (Figure 3d-f). 23:41 UTC is also the time at which the anvil convection began initiating its own lightning. As the new line of storms continued propagating eastward, a segment eventually bowed out and produced severe winds reported by Storm Data (May 2012).

B. Anvil flashes during the development of secondary convection

The first flash that propagated far into the anvil occurred at 23:12 UTC. It began near the southeast edge of the deeper reflectivity of the parent storm and extended eastward at an altitude of ~7 km above mean see level (MSL). The downward bulge and “fingers” in the reflectivity signature associated with the precursor of secondary convection, as noted in section 3.1, were collocated with the eastern end of the flash. Subsequent anvil flashes had initiation locations and propagation patterns similar to those of the first. The second and third anvil flashes produced by the Kingfisher storm both occurred between 23:23-23:25 UTC. The first echoes in the incipient secondary convection with Z ⩾ 18 dBZ visible in base scan data (0.5° radar elevation) appeared at 23:28 UTC, shortly after these two flashes.

The fourth anvil flash, at 23:34 UTC, differed slightly from the previous three. It began farther into the anvil, outside the base-scan reflectivity of the parent storm, and propagated eastward in two distinct levels, at 12 km and 7 km MSL(Figure 6b). The end point of the flash was the same as that of the first three; it propagated to the southernmost tip of the developing secondary convection. The reflectivity in the secondary convection had deepened by this time (Figure 4c) and maxima in one region had increased to ⩾50 dBZ, although that region of the secondary convection was north of the flash's end point.

The fifth anvil flash, at 23:40 UTC, was structured like the first three. A vertical cross section of reflectivity at 23:37 UTC indicates that the anvil convection had strengthened enough by then that rain was reaching the ground (not shown). Additionally, the fifth anvil flash occurred approximately one minute before the anvil convection began producing its own lightning.

All but the fourth of these flashes had NLDN-detected negative cloud-to-ground (CG) flashes associated with them. Most of these CGs occurred near the flash initiation points, which were at the eastern edge of Kingfisher storm in base-scan reflectivity. However, the fifth flash had a total of four CGs associated with it, and two of these were detected at least 20 km east of the Kingfisher storm, under the anvil.

C. Anvil lightning initiated by the secondary convection

The secondary anvil convection initiated its first flash at 23:41 UTC. That flash began at the northern end of the line of secondary convection and propagated southeast along the line (Figures 3d and 4d). There were deep, persistent reflectivity maxima evident in the vertical cross section of reflectivity at this time (Figure 4d). Following that flash, lightning activity continued in the secondary convection. Flashes were less frequent in the secondary convection than in the Kingfisher storm, but the Kingfisher storm was a maturing supercell and the secondary convection was still early in its developmental stage.

Many other anvil flashes were initiated by the secondary convection before it moved eastward beyond the Kingfisher storm's anvil. These were more variable in size, shape, and propagation pattern than the five initiated at the edge of the parent storm during the development of the secondary convection. The flashes themselves will not be addressed individually in this paper, although they were used to infer the charge structure of the anvil after the secondary convection began producing lightning, as discussed in the next section.

D. The source and location of the charge involved in anvil lightning

The charge structure inferred from lightning in the Kingfisher storm anvil included at least two horizontally extensive layers: a layer of positive charge centered at ~11 km MSL and a layer of negative charge centered at ~6-7 km MSL (e.g. Figure 6 (b)). This charge structure persisted after the secondary convection moved off the surface outflow boundary and remained consistent through 00:00 UTC.

The horizontal winds in the Kingfisher storm's anvil region between ~5-12 km MSL varied from westerly to west-northwesterly (i.e., blew from the west or northwest), as the predominantly westerly environmental winds had to circumvent the storm's updraft region. Because the horizontal wind patterns blew from the updraft and deeper convection of the parent storm into the anvil, the initial interpretation was that the charge in the anvil was advected from the parent storm (DiGangi 2014). Upon closer inspection of the storm's charge distribution, however, it became clear that charge advection could not be the source of all charge in the anvil. The charge inferred from several flashes in the parent Kingfisher storm included a positive charge layer at ~8 km MSL and a negative charge layer at ~12 km MSL, a configuration opposite in polarity at each level to the charge distribution inferred in the anvil, away from the parent storm. Charge regions inferred from flashes adjacent to each other in time and space demonstrate this discontinuity in the charge distribution (e.g., see Figures 7-9). The inferred charge structure of the secondary convection appeared to match the anomalous charge structure in the anvil away from the deep convection, except the charge distribution of the secondary convection also had an upper negative region (Figures 8-9).

We offer three hypotheses for the source of anomalous charge distribution in the anvil: 1) Opposing screening layer charges formed on the upper and lower anvil cloud boundaries; 2) Charge was generated locally in the anvil; 3) Charge in the anvil was produced by some combination of the two.

Though some charge advection from the parent storm was likely taking place, particularly in the western portion of the anvil, and screening layers may have formed, we infer from the observation that secondary convection within the anvil eventually generated its own frequent lightning that local charge generation was the primary source of charge in the eastern part of the anvil. The distribution of charge in the secondary convection further supports this conclusion: three layers of charge were inferred from flashes within the secondary convection, and the lower two of these were at approximately the same altitudes as the two charge layers inferred from anvil flashes propagating between the Kingfisher storm and the secondary convection (Figures 7-9). In addition to the formation of deep secondary convection being coincident with the first anvil flash initiated by the Kingfisher storm, all five anvil flashes occurring before the secondary convection initiated lightning propagated through approximately the same region of the anvil and terminated at the southern end of the secondary convection. This suggests to us that the charge in that portion of the anvil was related to the secondary convection.

We speculate that the vertical motion associated with the secondary convection was likely generating charge slowly as the convection developed, but produced enough charge that the interactions between those layers of charge and the charge produced in the Kingfisher storm could initiate large, horizontally extensive flashes. The mechanism for secondary anvil convection in this case was most likely that proposed by Knight et al. (2004): evaporative cooling of air as ice crystals and melted particles fall out of the anvil into the unsaturated air beneath the anvil causes localized destabilization, which can initiate convection. Weiss et al. (2012) suggested that for this mechanism to work in a real thunderstorm anvil, there must be a preexisting source of weak updraft collocated with the precipitation falling from the anvil. For the Kingfisher case, the leading edge of the outflow boundary visible in Figure 1 forced vertical ascent locally. The fact that the outflow boundary spanned the north-south extent of the anvil implies that vertical motion resulting from it would also have occurred throughout the north-south extent of the anvil while the outflow propagated, thus providing the impetus for localized charging in the anvil.

That subsequent anvil flashes maintained the same charge structure and occurred in roughly the same region as the previous anvil flashes suggests there was still localized charging occurring in the anvil after the secondary convection moved away from the rest of the anvil. One possibility is that the outflow boundary which initiated the secondary convection stalled under the anvil after 23:41 UTC (e.g. Figure 1), so the Knight et al. (2004) mechanism may still have supplied weak updrafts for local noninductive charging in the anvil after the secondary convection moved off the boundary.

IV. Summary and Conclusions

Secondary convection formed beneath the downshear anvil of the 29 May 2012 Kingfisher supercell observed during the DC3 field project. It appears to have been caused by destabilization of the local environment from ice crystals falling out of the anvil and cooling the air above an outflow boundary, thus enhancing the vertical motion at the leading edge of the boundary. The storm produced many anvil flashes following the initiation of the secondary convection.

The secondary convection began producing its own lightning about 30 minutes after convective initiation was diagnosed by WDDS-II. The continuity in inferred charge structure between the Kingfisher anvil lightning and the lightning in the secondary convection, coupled with discontinuities in the inferred charge layers between the anvil and the Kingfisher storm core, support the conclusion that updrafts associated with the outflow boundary and the Knight et al. (2004) mechanism in the anvil produced localized noninductive charging and macro-scale charge separation in the Kingfisher storm's anvil. After the secondary convection moved off the boundary, the boundary stalled beneath the anvil, and thus, may have maintained the presence of vertical motion strong enough to support active charging in the anvil cloud, consistent with the anvil charge structure persisting as observed.

Convection which forms within the anvils of supercell storms poses a threat to aircraft operating in the vicinity of thunderstorms, as well as to the general public. Secondary convection is difficult to predict in anvils because a previously formed, on-going storm is responsible for producing it. Furthermore, it is embedded within the anvil cloud and so is not initially visible in satellite data, and the proximity of its formation to a much stronger storm makes it easy to be overlooked by forecasters in radar data. Lightning mapping observations can serve as a useful flag in this situation to draw the attention of forecasters to the formation of a new storm hazard.

References

Barth, M. C., et al., 2015: Overview of the Deep Convective Clouds and Chemistry (DC3) field campaign. Bull. Amer. Meteor. Soc., 96, 1281-1309, doi: 10.1175/BAMS-D-13-00290.1.

Bluestein, H. B., and D. R. MacGorman, 1998: Evolution of cloud-to-ground lightning characteristics and storm structure in the Spearman, Texas tornadic supercells of 31 May 1990. Mon. Wea. Rev., 126, 1451-1467.

Bruning, E. C., W. D. Rust, D. R. MacGorman, M. I. Biggerstaff, and T. J. Schuur, 2010: Formation of charge structures in a supercell. Mon. Weather Rev., 138, 3740–3761, doi:10.1175/2010MWR3160.1.

Byrne, G. J., A. A. Few, and M. F. Stewart, 1989: Electric field measurements within a severe thunderstorm anvil. J. Geophys. Res. Atmos., 94, 6297–6307.

Coleman, L. M., T. C. Marshall, M. Stolzenburg, T. Hamlin, P. R. Krehbiel, W. Rison, and R. J. Thomas, 2003: Effects of charge and electrostatic potential on lightning propogation. J. Geophys. Res., 108, 4298, doi:10.1029/2002JD002718.

Crum, T. D., and R. L. Alberty, 1993: The WSR-88D and the WSR-88D Operational Support Facility. Bull. Am. Meteorol. Soc., 74, 1669–1687.

Cummins, K. L., and M. J. Murphy, 2009: An overview of lightning locating systems: History, techniques, and data uses, with an in-depth look at the U.S. NLDN. IEEE Trans. Electromagentic Compatibility, 51, 499–518.

DiGangi, E., 2014: *A Study of the Electrical, Kinematic, and Microphysical Properties of the 29 May 2012 Kingfisher Supercell*. M.S. thesis, School of Meteorology, The University of Oklahoma, 106 pp., URL http://hdl.handle.net/11244/14246.

Dye, J. E., and J. C. Willett, 2007: Observed enhancement of reflectivity and the electric field in long-lived Florida anvils. Mon. Weather Rev., 135, 3362–3380, doi:10.1175/MWR3484.1.

Dye, J. E., and Coauthors, 2007: Electric fields, cloud microphysics, and reflectivity in anvils of Florida thunderstorms. J. Geophys. Res. Atmos., 112, D11215, doi:10.1029/2006JD007550.

Herzog, B., 2013: *Total Lightning Information in a 5-Year Thunderstorm Climatology*. M.S. thesis, School of Meteorology, The University of Oklahoma, 114 pp.

Kasemir, H. W., 1960: A contribution to the electrostatic theory of a lightning discharge. J. Geophys. Res., 65, 1873–1878.

Knight, C. A., L. Jay Miller, and W. D. Hall, 2004: Deep convection and "first echoes" within anvil precipitation. Mon. Weather Rev., 132, 1877–1890.

Kuhlman, K. M., D. R. MacGorman, M. I. Biggerstaff, and P. R. Krehbiel, 2009: Lightning initiation in the anvils of two supercell storms. Geophys. Res. Lett., 36, L07802, doi:10.1029/2008GL036650.

Lakshmanan, V., T. Smith, G. Stumpf, and K. Hondl, 2007: The Warning Decision Support System–Integrated Information. Weather Forecast., 22, 596–612, doi:10.1175/WAF1009.1.

Lund, N. R., D. R. MacGorman, T. J. Schuur, M. I. Biggerstaff, and W. D. Rust, 2009: Relationships between lightning location and polarimetric radar signatures in a small mesoscale convective system. Mon. Weather Rev., 137, 4151–4170, doi:10.1175/2009MWR2860.1.

MacGorman, D. R., A.A. Few, and T.L. Teer, 1981: Layered lighting activity. J. Geophys. Res., 86, 9900-9910.

——, D. W. Burgess, V. Mazur, W. D. Rust, W. L. Taylor, and B. C. Johnson, 1989: Lightning rates relative to tornadic storm evolution on 22 May 1981. J. Atmos. Sci., 46, 221–251.

—— and W. D. Rust, 1998: *The Electrical Nature of Storms*. Oxford University Press, 422 pp.

——, J. M. Straka, and C. L. Ziegler, 2001: A lightning parameterization for numerical cloud models. J. Appl. Meteorol., 40, 459–478.

——, D. Rust, T. Schuur, M. Biggerstaff, J. Straka, C. Ziegler, E. Mansell, E. Bruning, K. Kuhlman, N. Lund, N. Biermann, C. Payne, L. Carey, P. Krehbiel, W. Rison, K. Eack, W. Beasley, 2008: TELEX The Thunderstorm Electrification and Lightning Experiment. Bull. Am. Meteorol. Soc., 89, 997–1013, doi:10.1175/2007BAMS2352.1.

Marshall, T. C., W. D. Rust, W. P. Winn, and K. E. Gilbert, 1989: Electrical structure in two thunderstorm anvil clouds. J. Geophys. Res. Atmos., 94, 2171–2181.

Mazur, V., 1989: A physical model of lightning initiation on aircraft in thunderstorms. J. Geophys. Res. Atmos., 94, 3326–3340.

Rison, W., R. J. Thomas, P. R. Krehbiel, T. Hamlin, and J. Harlin, 1999: A GPS-based three-dimensional lightning mapping system: Initial observations in central New Mexico. Geophys. Res. Lett., 26, 3573–3576.

Rust, W.D., W.L. Taylor, D.R. MacGorman, and R.T. Arnold, 1981: Research on electrical properties of severe thunderstorms in the Great Plains. Bull. Amer. Meteor. Soc., 62, 1286-1293.

——, D. R. MacGorman, E. C. Bruning, S. A. Weiss, P. R. Krehbiel, R. J. Thomas, W. Rison, T. Hamlin, and J. Harlin, 2005: Inverted-polarity electrical structures in thunderstorms in the Severe Thunderstorm Electrification and Precipitation Study (STEPS). Atmos. Res., 76, 247–271, doi: 10.1016/j.atmosres.2004.11.029.

Schuur, T. J., and S. A. Rutledge, 2000: Electrification of stratiform regions in Mesoscale Convective Systems. Part II: Two-dimensional numerical model simulations of a symmetric MCS. J. Atmos. Sci., 57, 1983–2006.

Stolzenburg, M., T. C. Marshall, W. D. Rust, and B. F. Smull, 1994: Horizontal distribution of electrical and meteorological conditions across the stratiform region of a Mesoscale Convective System. Mon. Weather Rev., 122, 1777–1797.

Takahashi, T., and K. Miyawaki, 2002: Reexamination of riming electrification in a wind tunnel. J. Atmos. Sci., 59, 1018–1025.

Thomas, R. J., P. R. Krehbiel, W. Rison, S. J. Hunyady, W. P. Winn, T. Hamlin, and J. Harlin, 2004: Accuracy of the Lightning Mapping Array. J. Geophys. Res. Atmos., 109, D14207, doi:10.1029/2004JD004549.

Weiss, S. A., D. R. MacGorman, and K. M. Calhoun, 2012: Lightning in the anvils of supercell thunderstorms. Mon. Weather Rev., 140, 2064–2079, doi:10.1175/MWR-D-11-00312.1.

Wiens, K. C., S. A. Rutledge, and S. A. Tessendorf, 2005: The 29 June 2000 supercell observed during STEPS. Part II: Lightning and charge structure. J. Atmos. Sci., 62, 4151–4177, doi:10.1175/JAS3615.1.

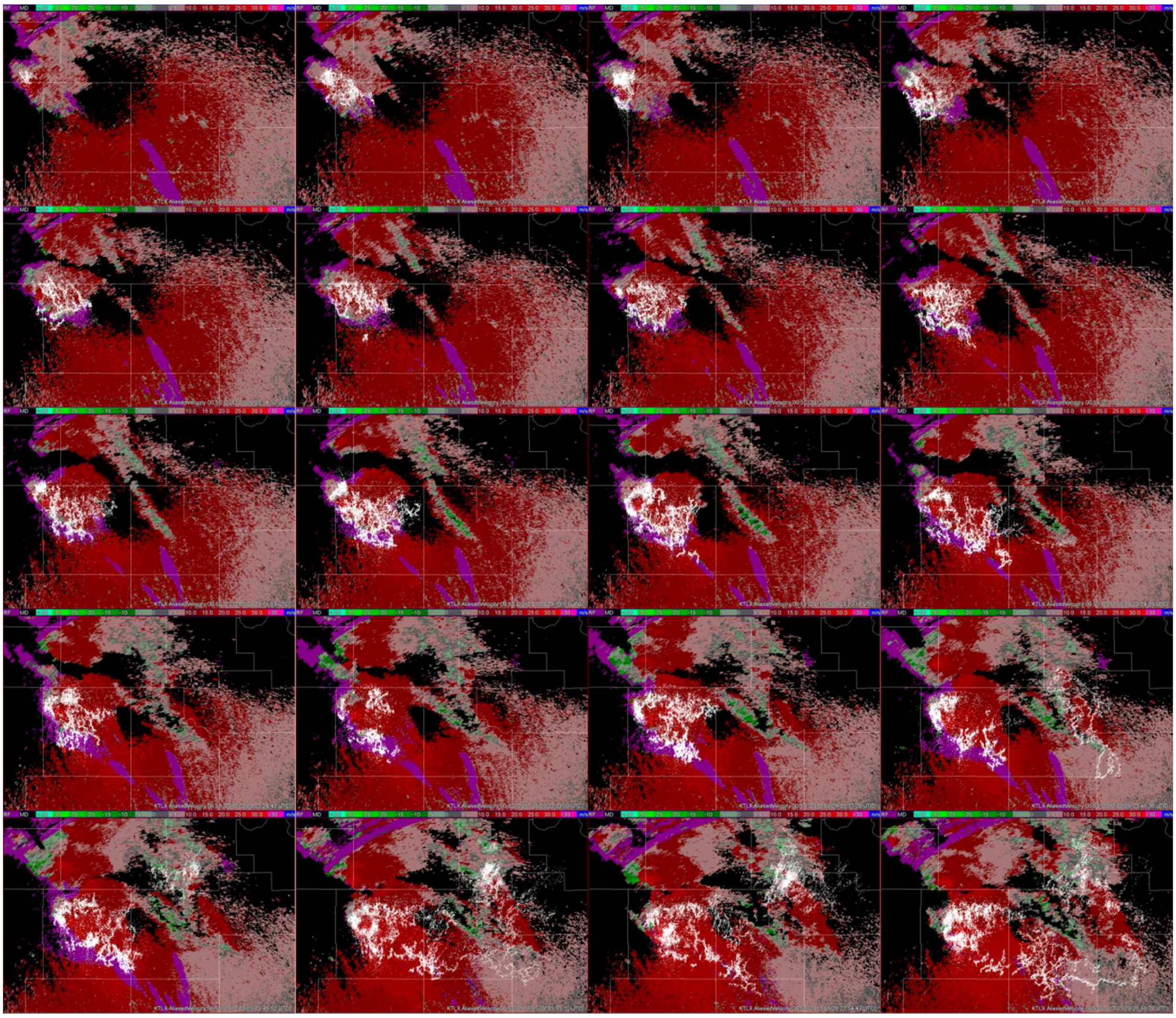

Figure 1: KTLX radial velocity (without alias correction) at the lowest tilt (0.5° elevation) for every volume scan (mostly at 4−6 min intervals) of the Kingfisher supercell from ~22:36 UTC on 29 May 2012 to ~00:00 UTC on 30 May 2012.

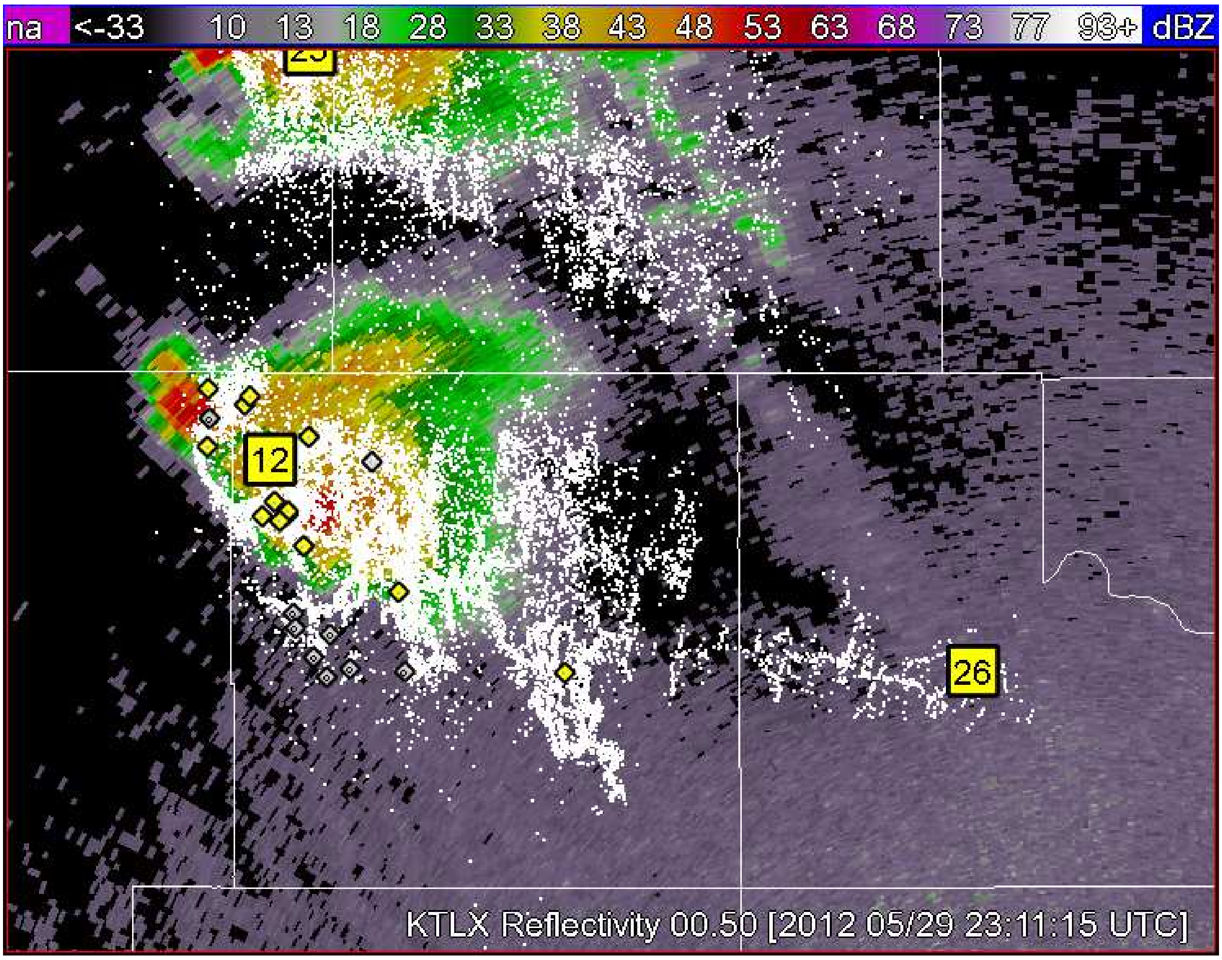

Figure 2: KTLX reflectivity at 23:11:15 UTC overlaid with one minute of VHF source points beginning at 23:12:00 UTC for the Kingfisher storm. Secondary convective initiation in the Kingfisher storm's anvil was detected by the WDSS-II w2segmotionll algorithm, denoted by the "26" marker. The first anvil flash propagating to the secondary convection occurred at almost the same time as convective initiation.

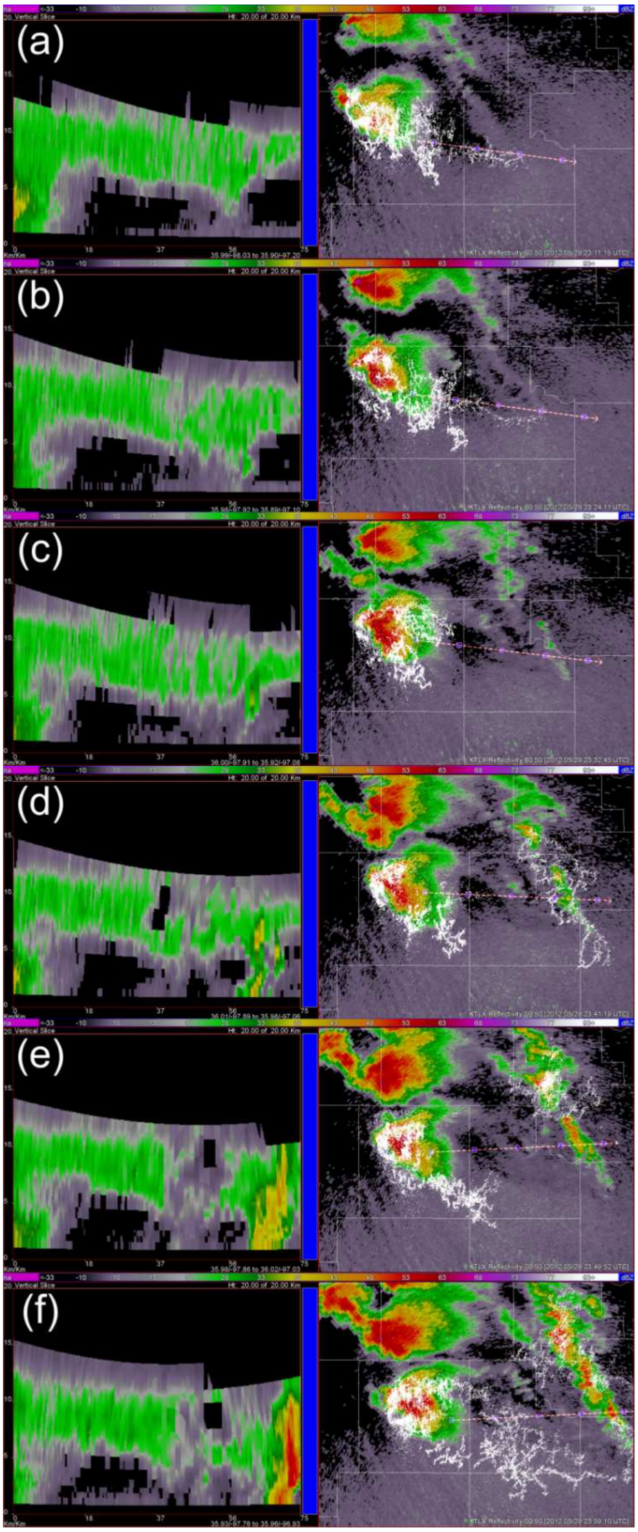

Figure 3(a-f): Vertical cross-sections of reflectivity out to the secondary convection and lightning superimposed on base scan reflectivity for KTLX volume scans beginning at (a) 23:11:15 UTC, (b) 23:24:11 UTC, (c) 23:32:45 UTC, (d) 23:41:19 UTC, (e) 23:49:52 UTC, and (f) 23:59:10 UTC. Some flashes propagated through these vertical cross sections. Overlaid VHF sources occurred during the one-minute period following the start of each volume scan (e.g., during 23:12:00-23:12:59 in panel a).

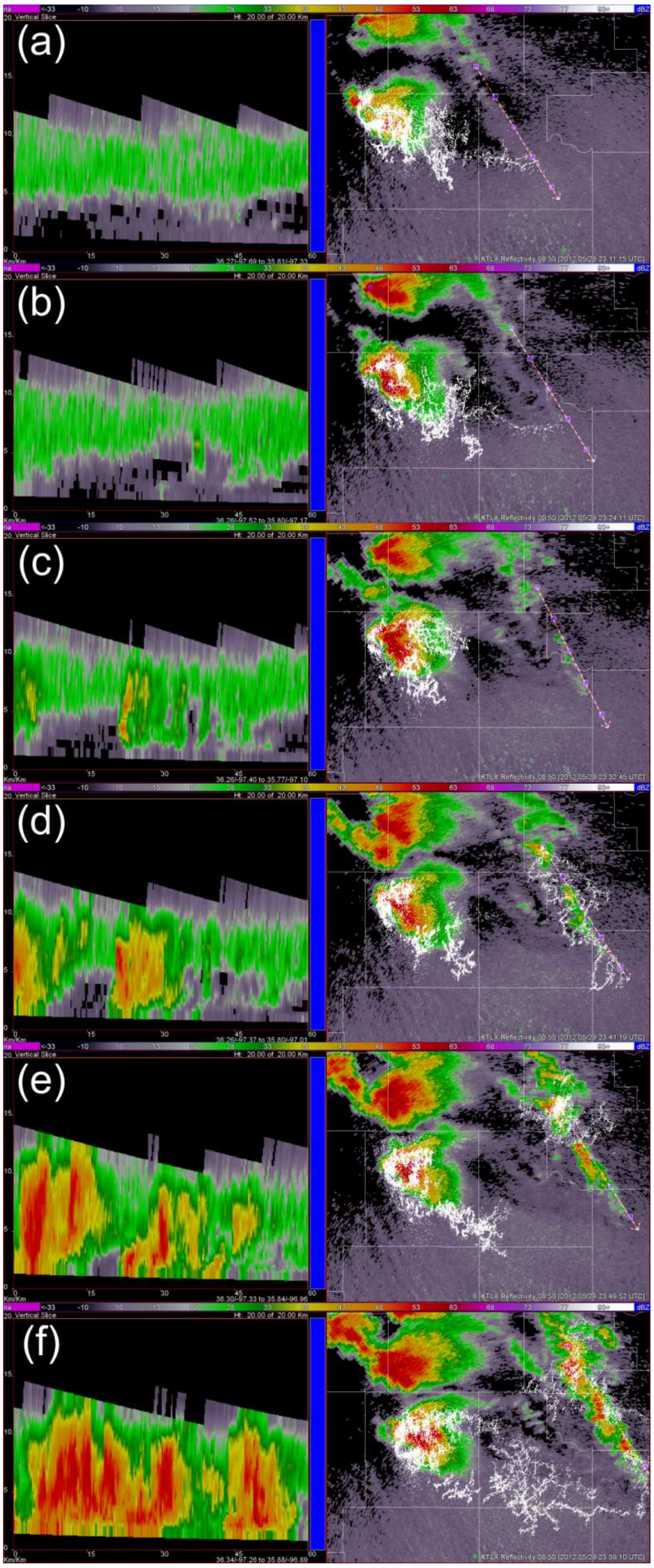

Figure 4(a-f): Vertical cross-sections of reflectivity with overlaid VHF sources along the boundary where secondary convection initiated and developed at the same times as in Figure 5.

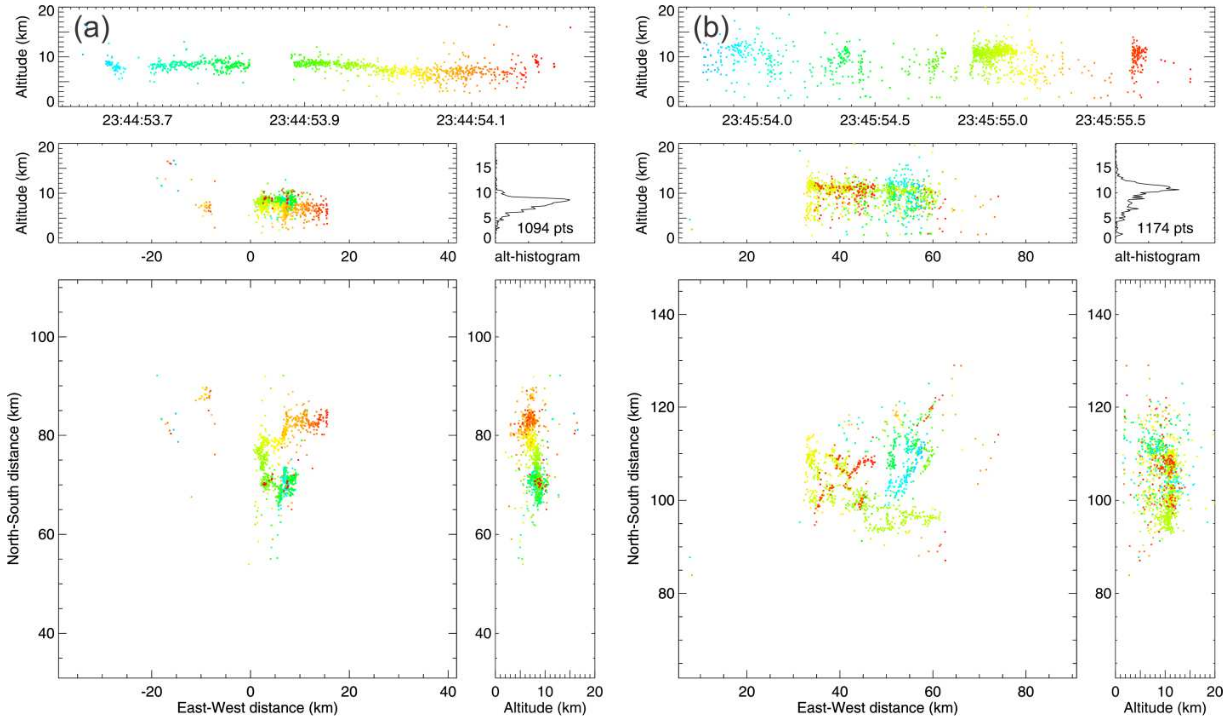

Figure 5: Individual flashes from a) (left) the Kingfisher storm at 23:44:53 UTC and b) (right) a flash from the secondary anvil convection at 23:45:53 UTC. VHF source points are colored by time.

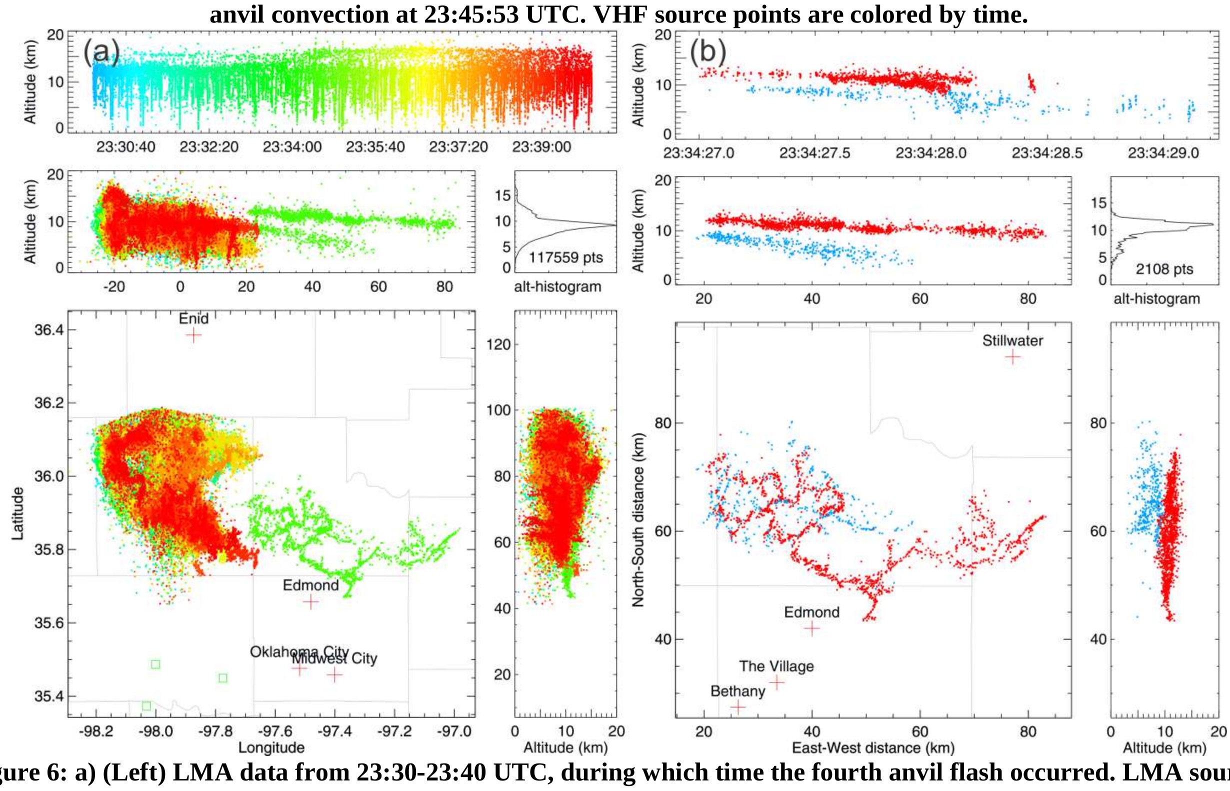

Figure 6: a) (Left) LMA data from 23:30-23:40 UTC, during which time the fourth anvil flash occurred. LMA sources colored by time. (b) (Right) The fourth anvil flash. LMA sources colored by the polarity of charge through which the leaders propagated: red indicates an inferred region of positive charge, and blue indicates an inferred region of negative charge.

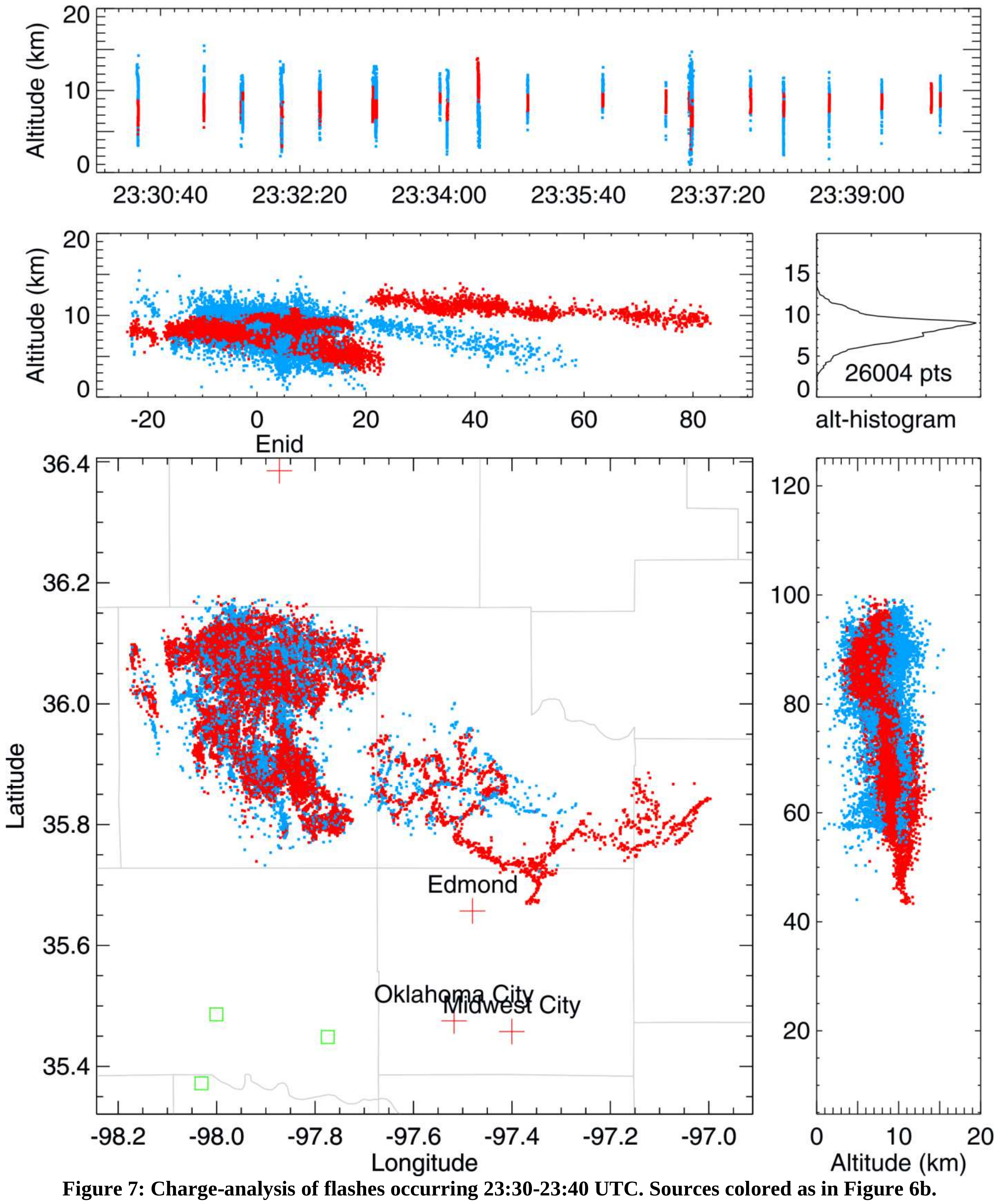

Figure 7: Charge-analysis of flashes occurring 23:30-23:40 UTC. Sources colored as in Figure 6b.

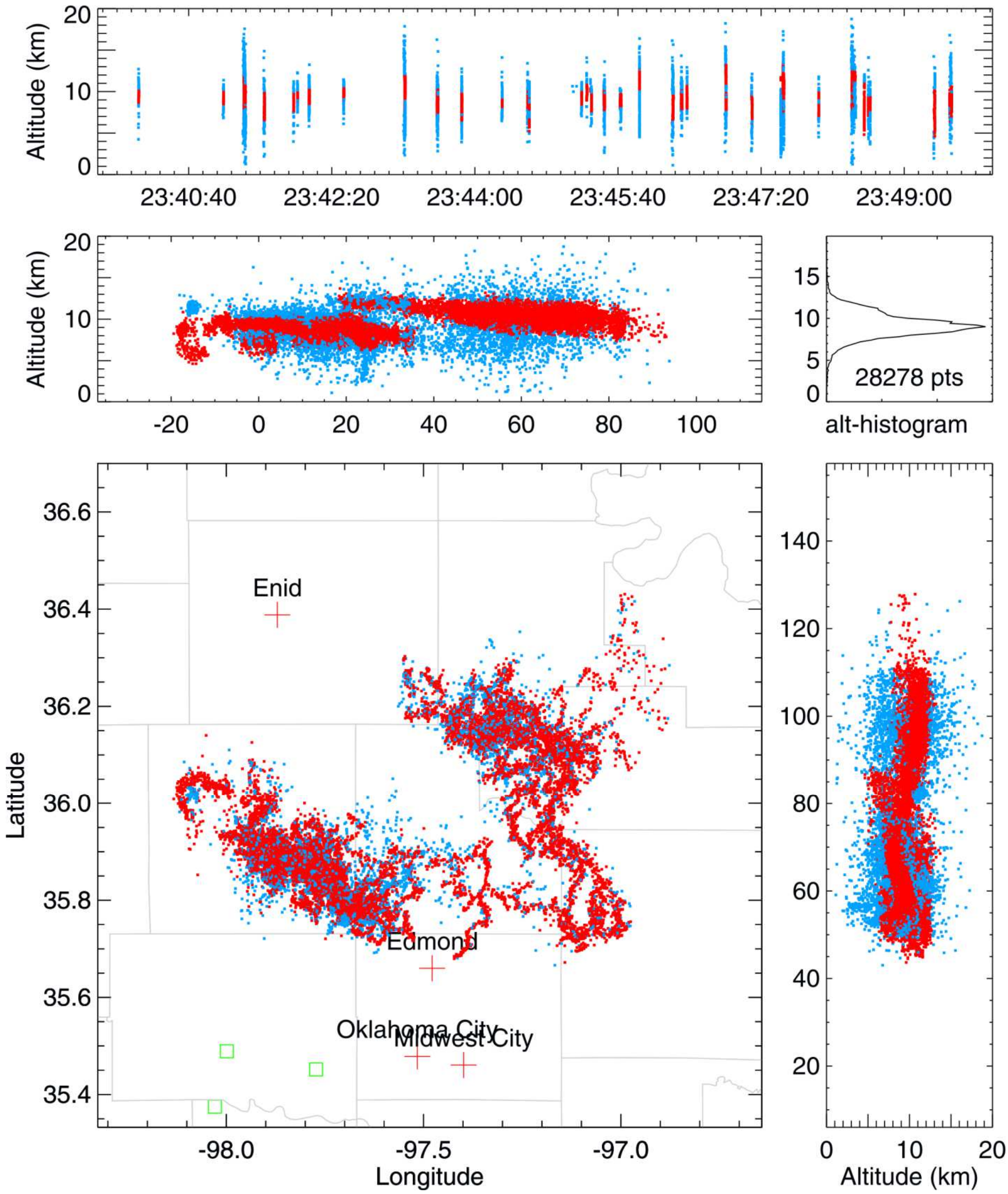

Figure 8: Charge-analyzed flashes between 23:50-23:50 UTC. Sources colored as in Figure 6b.

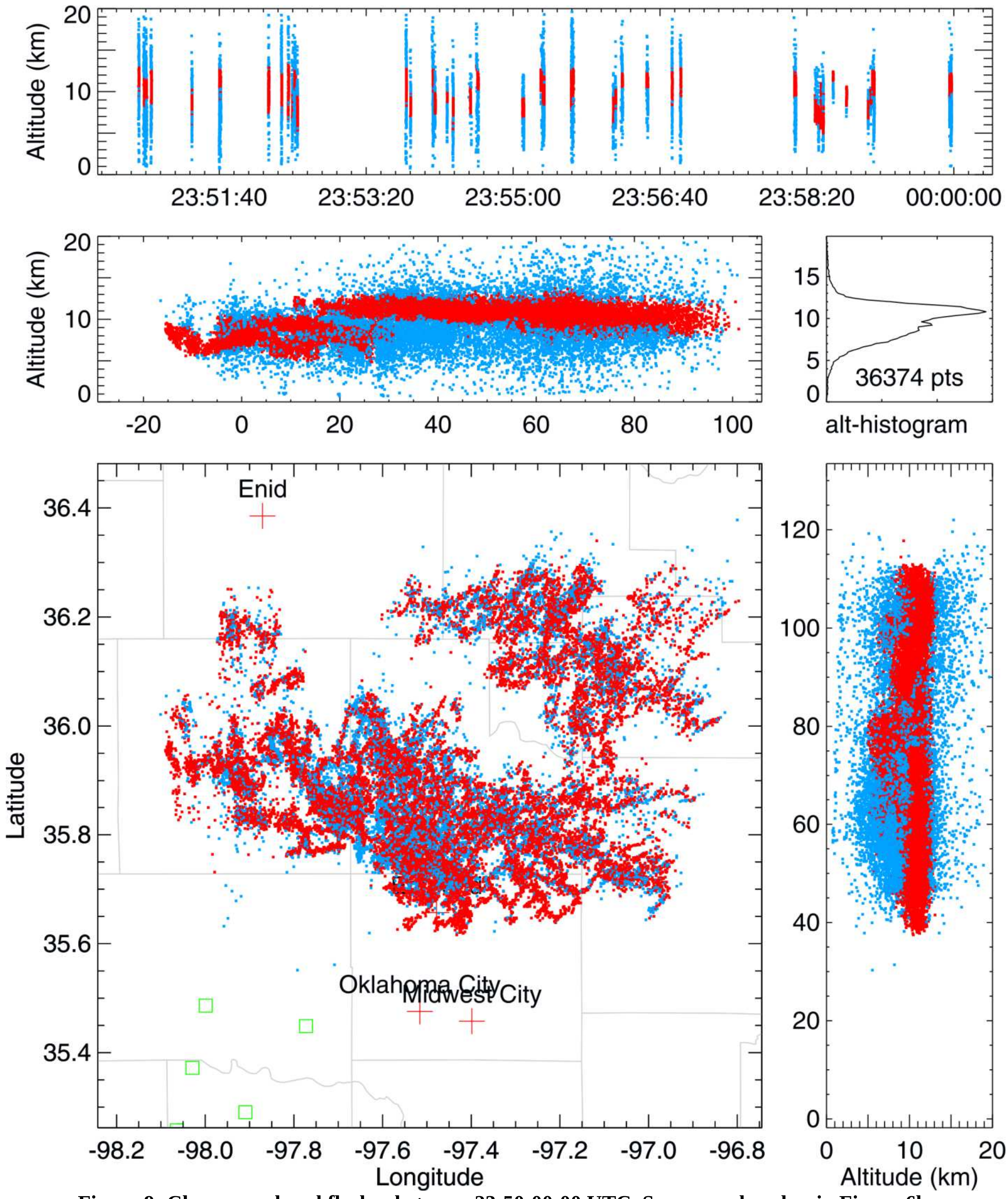

Figure 9: Charge-analyzed flashes between 23:50-00:00 UTC. Sources colored as in Figure 6b.